

Affinity-Based Purification of Polyisocyanopeptide Bioconjugates

Roel Hammink,^{†,§,#} Loek J. Eggermont,^{§,#} Themistoklis Zisis,^{†,‡} Jurjen Tel,^{§,||} Carl G. Figdor,[§] Alan E. Rowan,[†] and Kerstin G. Blank^{*,†,⊥}

[†]Department of Molecular Materials, Institute for Molecules and Materials, Radboud University, Heyendaalseweg 135, 6525 AJ Nijmegen, The Netherlands

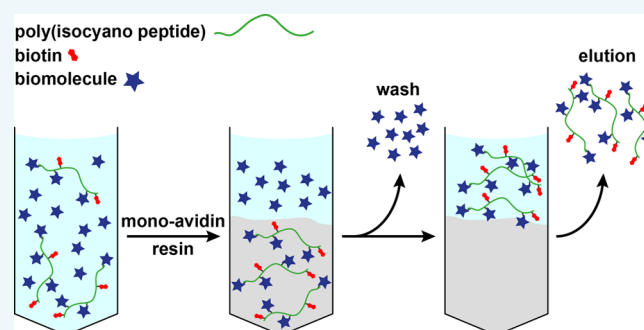
[§]Department of Tumor Immunology, Radboud Institute for Molecular Life Sciences, Radboud University Medical Center, Geert Grootplein 26, 6525 GA Nijmegen, The Netherlands

^{||}Department of Biomedical Engineering and Institute for Complex Molecular Systems, Laboratory of Immunoengineering, Eindhoven University of Technology, De Zaal 15, 5612 AP Eindhoven, The Netherlands

[⊥]Mechano(bio)chemistry, Max Planck Institute of Colloids and Interfaces, Potsdam-Golm Science Park, 14424 Potsdam, Germany

Supporting Information

ABSTRACT: Water-soluble polyisocyanopeptides (PICs) are a new class of synthetic polymers that mimic natural protein-based filaments. Their unique semiflexible properties combined with a length of several hundred nanometers have recently enabled a number of biomedical applications ranging from tissue engineering to cancer immunotherapy. One crucial step toward the further development of PICs for these applications is the efficient and controlled synthesis and purification of PIC–biomolecule conjugates. Considering the large size of PICs and the biomolecules to be conjugated, conjugation reactions do usually not proceed to completion due to steric effects. As a consequence, purification of the reaction mixture is necessary to separate the obtained bioconjugates from unreacted biomolecules. As a direct result of the semiflexible nature of PICs, standard polymer and protein purification methods based on molecular weight have not been successful. Here, we introduce a new affinity-based purification method utilizing biotin as an affinity tag. PICs decorated with a controlled and tunable density of biotin molecules (biotinPICs) were efficiently bound to and eluted from a monoavidin resin in buffered aqueous solution. Using these biotinPICs, two different protein conjugates were synthesized, one carrying the enzyme alkaline phosphatase (PhoA) and the other T-cell activating anti-CD3 antibodies. The resulting biotinPIC–protein conjugates were successfully obtained in high purity (>90%) and without any loss of protein activity. The high purity greatly simplifies the analysis of biotinPIC bioconjugates, such as the determination of the average number of biomolecules conjugated per biotinPIC chain. Most importantly, it allows for the direct and straightforward application of the obtained bioconjugates in the desired applications. The new method developed may further be adapted for the purification of other advanced bioconjugates that are difficult to obtain in high purity with the available standard methods.



INTRODUCTION

Following the synthesis of the first polymer–protein conjugate approximately 40 years ago,¹ the range of applications of these functional bioconjugates has grown enormously. The first and still most-common motivation for the synthesis of polymer–protein conjugates is to improve the properties of therapeutic proteins. Nowadays, the conjugation of poly(ethylene glycol) (PEG) is a frequently employed strategy to increase protein solubility and stability, to reduce immunogenicity and to alter circulation half-life.^{2–4} With continuous improvements in polymer synthesis and bioconjugation methods,^{5–8} the range of applications has expanded and new classes of polymers have been utilized. For example, conjugation with stimuli-responsive polymers such as poly(*N*-isopropylacrylamide) (PNIPAAm) introduces additional functionality into the protein.^{5,8,9} Making use of the temperature-sensitive behavior of PNIPAAm, the

protein–polymer conjugate reversibly precipitates when increasing the temperature above the lower critical solution temperature (LCST) of PNIPAAm,⁵ allowing for the development of advanced purification methods and diagnostic assays.^{8,9} Linear or branched polymers with multiple reactive groups have been used as scaffolds for the synthesis of multivalent bioconjugates with increased binding strength^{10–14} or of multifunctional entities that combine different activities.^{12,13,15} The latter is of particular interest for engineering enzyme cascades in which the reaction intermediates need to be efficiently transferred between enzyme active sites.^{15–17} Polymer bioconjugates further find application for the synthesis

Received: July 10, 2017

Revised: August 24, 2017

Published: August 28, 2017

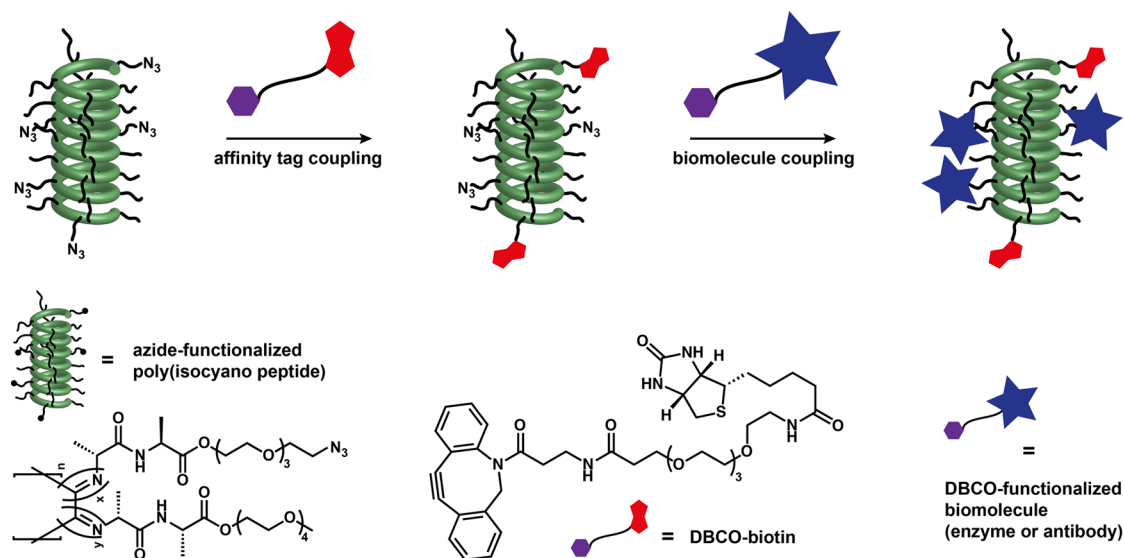


Figure 1. Conjugation strategy for the synthesis of biotin-functionalized polyisocyanopeptides that can be used for the subsequent coupling of DBCO-containing biomolecules. In this work, the biomolecule is either an antibody (α CD3) or an enzyme (PhoA).

of biocompatible hydrogels for tissue-engineering applications^{18–21} as well as for the synthesis of self-assembled nanostructures, in which the biomolecules are used as functional material building blocks.^{22,23}

Over the last few years, we have introduced water-soluble polyisocyanopeptides (PICs) as novel and versatile polymer scaffolds for biological applications.^{24–26} PICs are long (100–1000 nm) and semiflexible polymers that mimic the properties of many protein-based filaments found in nature, e.g., in the cytoskeleton and the extracellular matrix. Their semiflexibility is a direct result of their helical secondary structure and represents a unique feature for synthetic polymers.^{27,28} PICs are polymerized from isocyanide monomers that carry a short dialanine peptide in every monomer. Upon folding into a helix, hydrogen bonds between the peptide amides stabilize the helical structure. PIC monomers are further functionalized with oligoethylene glycol chains to provide water solubility. When carrying a triethylene glycol chain (EG₃), the corresponding PIC undergoes a sol-to-gel transition at a temperature of ~ 19 °C.^{27,29} Consequently, EG₃-functionalized PICs form a hydrogel at room temperature. This hydrogel has been used in cell culture²¹ and for sensing the binding of short oligonucleotides to their complementary sequence.³⁰ In contrast, tetraethylene glycol (EG₄) functionalized polymers undergo a sol-to-gel transition at 40–45 °C.²⁷ These PICs are therefore fully dissolved at physiologically relevant temperatures, making them excellent scaffolds for the synthesis of polymer conjugates. As a first application, we have attached T cell stimulating antibodies to EG₄-functionalized PICs and used these PIC–antibody conjugates as novel artificial antigen-presenting cells in immunotherapeutic applications.^{11,12,14}

All of these applications have in common that the PICs have to be functionalized with biomolecules. For the cell-culture application, a short integrin-binding GRGDS peptide was grafted onto PICs to provide cell adhesion sites in the hydrogel.²¹ In the sensing application, short DNA oligonucleotides were coupled to the PICs. These DNA sequences were subsequently cross-linked upon binding of an analyte.³⁰ For the immunotherapeutic application, the PICs were functionalized

with streptavidin to allow for the subsequent binding of biotinylated antibodies.^{11,12,14}

As a direct result of their unique physical properties, these semiflexible PICs do not form a typical random coil structure in solution. This complicates the separation of polymer–biomolecule conjugates from nonreacted biomolecules following a conjugation reaction. Despite careful optimization, neither dialysis nor size-exclusion chromatography or field flow fractionation methods were found to be successful. Ultrafiltration was identified as the only possible method for the purification of freshly synthesized PIC bioconjugates, but more than 99% of the material was lost during the process.^{11,12,14} As an alternative, the reaction between PICs and biomolecules was carefully optimized so that an almost quantitative coupling of biomolecules was achieved and no purification was needed. For small molecules, such as short peptides²¹ and DNA oligonucleotides,³⁰ this method was successful. For large proteins, e.g., antibodies, the reaction with the PIC is not quantitative,^{11,12,14} however, because steric effects limit the kinetics and the yield of the reaction. Clearly, an alternative and efficient purification method is needed to obtain pure PIC bioconjugates in good yield.

Affinity tags such as the hexahistidine tag,³¹ the strep-tag,³² or biotin³³ are frequently used for the purification of recombinantly expressed proteins from crude cell extracts. To the best of our knowledge, such a purification strategy has never been used for the purification of bioconjugates that contain a synthetic polymer. Inspired by the affinity tag method, a PIC polymer carrying biotin as an affinity tag was designed. Using this biotin-functionalized PIC (biotinPIC), affinity purification on a monoavidin resin can potentially be used to remove unreacted biomolecules. Monoavidin is a monomeric derivative of avidin that possesses a highly reduced affinity for biotin.³⁴ It has been shown that biotinylated molecules bind to monoavidin agarose in a reversible manner and can be eluted competitively when adding high concentrations of free biotin.³⁵ Here, we describe the synthesis and characterization of biotinPIC polymers. We show that these biotinPICs reversibly bind to a monoavidin resin and that this affinity purification method can be used for the purification of

biotinPIC bioconjugates. The versatility of this new purification method is demonstrated using two different model proteins, an antibody and an enzyme. The enzyme (alkaline phosphatase from *Escherichia coli*; PhoA) was chosen as it allows for the straightforward determination of the activity of the conjugated biomolecule. The antibody of choice is the same anti-CD3 antibody (α CD3) that has been used earlier for the synthesis of PIC–antibody conjugates for stimulating T cells.^{11,12,14}

RESULTS AND DISCUSSION

Synthesis and Characterization of Biotin-Functionalized Polyisocyanopeptides. To investigate if the biotin affinity tag can be used for the purification of PIC bioconjugates, biotin-functionalized polymers were synthesized (Figure 1) and used in a series of purification experiments. For this purpose, PICs containing azide-functionalized side chains in a predefined density were synthesized using the same method as described in our previous publications.^{11,12,14,21,30} In short, functional azide monomers were co-polymerized with monomers containing nonfunctional methoxy groups using a nickel catalyst. The ratio of azide to methoxy monomers was chosen to be 1:30, yielding a statistical average distance between azides of 3 nm. Subsequently, the azide-functionalized PIC was reacted with different relative amounts of biotin–azadibenzocyclooctyne (biotin–EG₄–DBCO) in a strain-promoted azide–alkyne cycloaddition (SPAAC) reaction.³⁶ Assuming a quantitative yield of the reaction, biotinPICs with an average biotin spacing of 5, 7.5, 10, and 40 nm were prepared. Using this strategy, the remaining azide groups are available for a second SPAAC reaction that allows for the coupling of DBCO-functionalized biomolecules.

To optimize the biotin density necessary to bind and elute the biotinPICs from monoavidin containing beads in a batch purification process, an incubation and elution protocol was developed. The polymers were diluted to 0.1–0.2 mg mL⁻¹ in phosphate-buffered saline (PBS) and mixed with a 50% slurry of monoavidin beads in a 1:1 (v/v) ratio. The binding of the biotinPICs to the beads was determined by measuring the concentration of unbound biotinPIC in the supernatant using circular dichroism (CD) spectroscopy. Due to the helical conformation of the PICs, this technique provides an indication of the polymer concentration, assuming that the polymer conformation is not altered during the experiment.^{25,26,37} The CD spectrum of the PIC is characterized by a negative peak at $\lambda = 360$ nm and a larger positive peak with a maximum at $\lambda = 272$ nm (Figure S1). Calibration curves of the azide-functionalized PIC were determined at both wavelengths, showing that the corresponding peak heights scale linearly with polymer concentration (Figure S1). The analysis of the supernatants after 4 h of incubation shows that the biotinPICs are able to bind to the monoavidin beads. When the samples with different biotin densities were compared, clear differences are seen in the fraction of bound biotinPICs (Figure 2a). Polymers with the lowest biotin density (spacing of 1 biotin per 40 nm) showed little binding (~12%) and the majority of biotinPICs remained in the supernatant. Decreasing the biotin spacing to 10 nm already increased the fraction of bound biotinPICs to ~30%. A further decrease in the biotin spacing to 7.5 and 5 nm allowed for binding ~65–70% of the biotinPICs to the monoavidin beads. The biotin spacing was not decreased further because a sufficient amount of free azides is required for further bioconjugation.

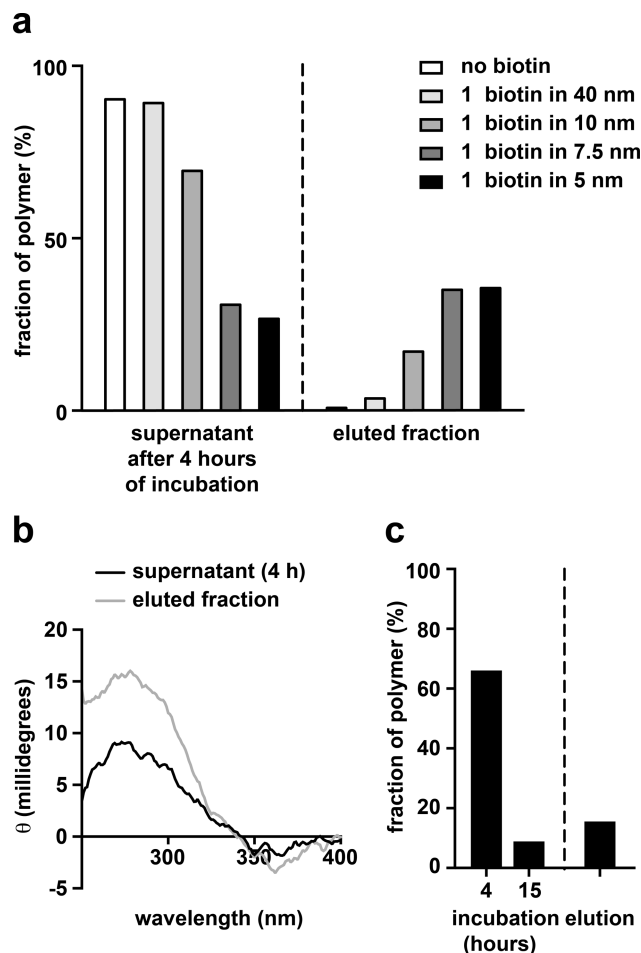


Figure 2. Binding and elution of biotinPICs to and from monoavidin beads. (a) Binding and elution profiles for biotinPICs containing a different biotin density (EG₄ linker). Shown is the relative amount of biotinPIC in the supernatant after binding or elution. (b) CD spectrum of the supernatant after 4 h of incubation. In addition, the eluted fraction is shown (data shown for 1 biotin in 7.5 nm). (c) Binding and elution profile of biotinPICs prepared with the long (3000 Da) PEG linker and a biotin spacing of 7.5 nm. Shown is again the relative amount of biotinPIC in the supernatant after binding and elution.

After the binding of the biotinPICs to monoavidin beads was confirmed, the elution protocol was optimized. The beads were first washed with PBS containing 0.1% Tween 20 (PBS-T, 2 \times) and PBS (4 \times) to remove any nonspecifically bound polymers. During this extensive washing protocol, ~30% of the beads were lost, which reduces the total yield of eluted polymers. Following washing, PBS containing 2 mM biotin was added to the beads to elute the bound biotinPICs competitively. In the last step, the eluate was filtered over a frit with 20 μ m pore size to remove residual monoavidin beads. The CD spectrum of the eluted fractions was not altered in comparison with the original polymer samples before purification, which indicates that the helical structure is not affected during the binding and elution process (Figure 2b). The fraction of eluted biotinPICs clearly correlates with the relative amount of biotinPIC initially bound to the beads and, consequently, also with the density of biotin coupled to the polymer. Only a small fraction (4% of the original amount) was obtained for the polymer with a biotin spacing of 40 nm. Higher fractions of 17, 34, and 35% were obtained for the other polymers with a biotin spacing of 10, 7.5,

and 5 nm, respectively (Figure 2a). Considering the loss of beads during the washing steps and the fraction of polymer that did not bind to the beads, elution with 2 mM biotin is sufficient to elute more than 50% of the bound biotinPIC polymers.

In addition to the biotin density, also the linker length between biotin and the PIC polymer backbone was investigated. To test for possible steric hindrance, the length of the PEG spacer between the biotin moiety and the DBCO functional group was increased. Using a PEG linker with a molecular weight of 3000 Da, biotinPIC polymers were prepared with an average biotin spacing of 7.5 nm. Binding of this polymer to the beads was considerably slower when compared with the previously used biotinPICs containing only the EG₄ linker. Only after 15 h of incubation more than 90% of the polymer was bound. Unfortunately, elution of this polymer recovered only 15% of the original amount (Figure 2c). Overall, it appears that the longer linker does not reduce but instead increases steric hindrance thereby affecting both the kinetics of the interaction and the yield of the purification protocol.

Taken together, these results show that the biotinPIC with a biotin spacing of 7.5 nm coupled via the short linker performs best when considering both the requirements for an efficient purification and its future application. It shows good binding and a reasonable amount is eluted from the monoavidin beads. At the same time, a sufficient number of azides is left for further conjugation. This biotinPIC was therefore selected as a model system to test whether this purification method can be used for the purification of biotinPIC bioconjugates.

Synthesis and Purification of Alkaline Phosphatase BiotinPIC Bioconjugates. To investigate if biotinPIC bioconjugates can be purified with the newly developed affinity-based method, biotinPICs were first functionalized with the enzyme PhoA. This was motivated by the availability of a large number of chromogenic and fluorogenic phosphoester substrates, which facilitate a straightforward comparison of enzyme activity before and after conjugation. To complement this sensitive activity readout, the enzyme was labeled with a fluorophore so that also the enzyme concentration can be determined easily during all steps of the experiment. PhoA was therefore reacted with the *N*-hydroxysuccinimide (NHS) esters of DBCO and AlexaFluor647 in a one-pot reaction. To determine the degree of labeling, the PhoA concentration was estimated with a bicinchoninic acid (BCA) assay and the DBCO and AlexaFluor647 concentrations were determined with UV–vis spectroscopy. On average, 1.1 fluorophore molecules and 2.4 DBCO functional groups were coupled to the PhoA dimer. DBCO- and AlexaFluor647-labeled PhoA was then reacted with the biotinPIC polymer possessing a biotin spacing of 7.5 nm. Three different ratios of PhoA:azide were used for coupling the enzyme to the polymer (0.1, 0.2, and 0.5 eq. of PhoA with respect to azide groups). Assuming a quantitative reaction, this would result in an average PhoA spacing of 50, 25, and 10 nm.

The PIC–PhoA bioconjugates were then purified over monoavidin beads, using the optimized method described earlier for biotinPICs. The purified PIC–PhoA conjugates were analyzed with atomic force microscopy (AFM). The AFM images were used to count the number of enzymes attached to every individual polymer chain (Figures 3a, b and S2) and the average spacing between PhoA molecules was determined to be 55 nm (PIC 0.2 eq PhoA) and 100 nm (PIC 0.1 eq PhoA). In parallel, the polymer concentration was determined in a CD measurement at a wavelength of 360 nm, and the PhoA

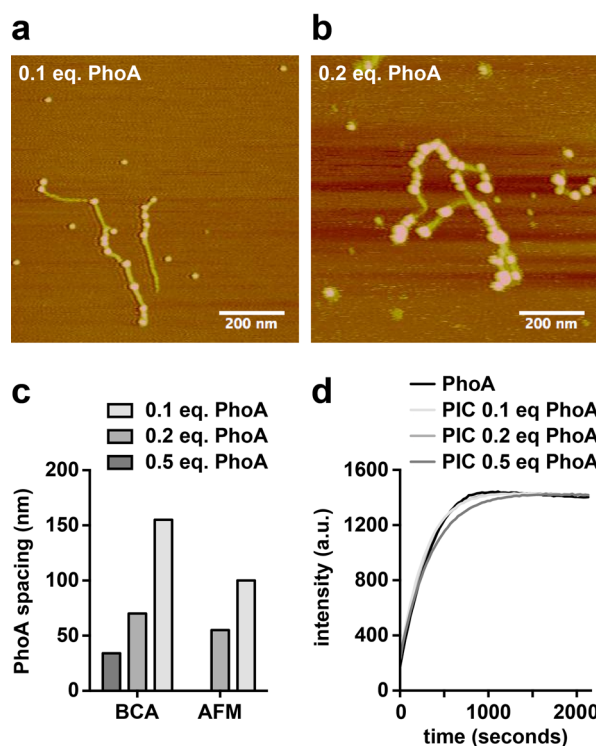


Figure 3. Synthesis and purification of biotinPIC–PhoA bioconjugates. (a,b) Atomic force microscopy (AFM) images of biotinPICs reacted with 0.1 equiv PhoA or 0.2 equiv PhoA drop-casted on mica. The bright “dots” correspond to the enzyme, while the “connecting line” represents the polymer. (c) Calculated PhoA distances on the biotinPIC backbone, determined either from the measured bulk concentrations (bicinchoninic acid assay, BCA) or the AFM measurement. (d) Enzyme activity measurements of the PIC–PhoA conjugates in comparison to nonconjugated PhoA. The curves display the mean of three independent measurements.

concentration was determined with a BCA assay. This measurement yielded a spacing of 70 nm for the biotinPIC functionalized with 0.2 eq. PhoA and of 155 nm for the biotinPIC functionalized with 0.1 eq PhoA (Figure 3c). Considering the error in the AFM-based estimation, these values agree very well. This proves that unreacted enzymes have been efficiently separated from the bioconjugates during the purification process. Unfortunately, no polymer bioconjugates were found on the mica surface for the biotinPIC functionalized with 0.5 eq PhoA, but the spacing determined from the bulk concentration assay was 34 nm. On average, the determined PhoA spacing is a factor of 3 larger than the distances expected for a quantitative reaction, indicating a coupling efficiency of 30%. This low coupling efficiency is expected for a reaction between two macromolecules and again highlights the importance of a good purification method.

In the next step, it was examined if the biotinPIC-conjugated PhoA was still catalytically active (Figure 3d). The activity of the enzyme was tested using the fluorogenic substrate 9H-(1,3-dichloro-9,9-dimethylacridin-2-one-7-yl) phosphate (DDAO–phosphate).³⁸ PhoA dephosphorylates the DDAO fluorophore, thereby altering its photophysical properties (Figure S3). Enzymatic activity results in an increase in product fluorescence allowing for a straightforward kinetic measurement. The increase in product fluorescence was determined for the three PIC–PhoA conjugates and for a control sample containing non-conjugated enzyme of the same concentration (determined

via the fluorescence intensity of the AlexaFluor647 label before the kinetic measurement was started). All samples show very similar enzyme activities (Figure 3d), indicating that the coupling and purification process does not inactivate the enzyme.

Taken together, these results show that the new purification protocol is a highly powerful method for the purification of PIC–enzyme conjugates. In the next step, these conjugates could be used for forming enzyme-functionalized hydrogels for a number of different applications. Such nature-like hydrogels represent an interesting new method for enzyme immobilization, as their large pore size²⁷ allows for free substrate and product diffusion. PIC polymers are further highly versatile scaffolds for the coconjugation of different functional entities¹² so that they represent an interesting new platform for the assembly of cascade reactions.

Synthesis and Purification of anti-CD3 BiotinPIC Bioconjugates. After the establishment that the new purification protocol can be used to purify PIC bioconjugates, an antibody was conjugated to the biotinPIC in the next step to investigate the general applicability of the method. This was further motivated by our earlier experiments with anti-CD3 (α CD3) functionalized PICs that were shown to be highly effective as synthetic dendritic cells.^{11,12,14} To obtain PIC- α CD3 of sufficient purity, the polymer conjugates had to be purified extensively using ultrafiltration, which resulted in a huge loss of both polymer and antibody (<1% yield). Therefore, using the previously utilized α CD3 antibody, it was tested if the new affinity-based purification method can overcome these problems and yield PIC- α CD3 bioconjugates with increased yield and purity. In the earlier experiments, α CD3 was biotinylated and bound to a streptavidin-functionalized PIC polymer. Because biotin is now used as the affinity tag for purification, the original design had to be adjusted to allow for a direct conjugation of α CD3 to the azide-functionalized biotinPIC. To achieve this, α CD3 was functionalized with the DBCO–NHS ester, allowing a direct conjugation to the biotinPIC. The degree of labeling, as determined by UV–vis spectroscopy,³⁹ was between 2 and 2.5 DBCO molecules per antibody.

To investigate the influence of the antibody density on the performance of the biotin-tag-based purification method, four different PIC- α CD3 bioconjugates were synthesized. DBCO- α CD3 was reacted with biotinPIC in PBS using 0.1, 0.3, 0.5, and 1 equiv of antibody relative to azide groups. The resulting reaction mixtures were then incubated with monoavidin beads. The ability of the PIC- α CD3 bioconjugates to bind to the resin was estimated by analyzing the supernatant with CD (Figures 4a and S1). The binding efficiency of the PIC- α CD3 to the monoavidin beads was typically in the range of 35–55%, which was lower than for the biotinPIC without α CD3 (65–70%). After extensive washing (2 \times PBS-T, 4 \times PBS), typically 10–25% of the original amount of PIC- α CD3 could be eluted (Figure 4a). Compared to biotinPIC without α CD3, these yields are slightly lower, which is a direct result of a less efficient capture of the bioconjugate. This may originate from steric effects resulting from the large antibody or less-favorable charge interactions between the antibody and monoavidin.⁴⁰ In the case of unfavorable charge interactions, optimizing the buffer conditions in the capture and/or release step may lead to increased yields in future experiments. Still, the yields are significantly better than the yields obtained with the ultrafiltration protocol used before (<1% yield).

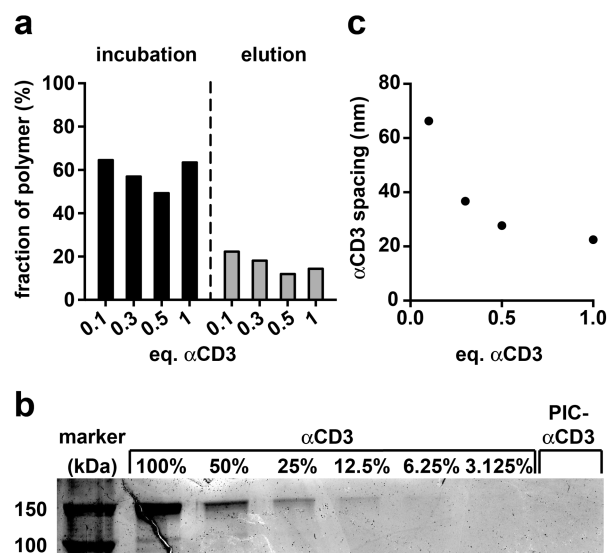


Figure 4. Purification of PIC- α CD3 bioconjugates using a biotin affinity tag. (a) Binding and elution profile of PIC- α CD3 to and from monoavidin agarose beads. Shown is the relative amount of PIC- α CD3 in the supernatant, determined using CD measurements. (b) Nonreducing SDS-PAGE of the PIC- α CD3 sample (1 equiv of antibody with respect to azide groups) in comparison with different concentrations of α CD3. Shown are relative concentrations with respect to the amount of α CD3 used in the reaction mixture. (c) Calculated average distances between α CD3 on the biotinPIC backbone obtained for different equivalents of DBCO- α CD3 during the reaction.

In addition to the yield, the purity of the PIC- α CD3 is also a crucial aspect for the further optimization and applicability of these bioconjugates. A combination of methods was used to determine the remaining amount of nonconjugated α CD3 in the samples after affinity purification. Sodium dodecyl sulfate polyacrylamide gel electrophoresis (SDS-PAGE) was performed under nonreducing conditions to keep the disulfide bonds of the antibody intact (Figure 4c). Because the polymer bioconjugate is too large to enter the SDS-PAGE gel (Figure S4), it can be directly concluded that any protein of the size of \sim 150 kDa represents nonconjugated antibody. A comparison of the PIC- α CD3 sample (1 equiv of antibody with respect to azide groups) with different concentrations of free α CD3 shows that more than 92% of the antibody in the affinity purified sample was conjugated to the polymer. This result is in line with the results obtained for the PIC-PhoA conjugates, in which only a very small amount of nonconjugated PhoA was observed in the AFM images (Figure 3). This high purity of the PIC- α CD3 conjugates allows for a simple determination of the number and the statistical spacing of α CD3 on the polymer backbone. Knowing the molar concentrations of both the antibody and the biotinPIC, the number of α CD3 per polymer can simply be determined by dividing the two values (Figure 4c). The biotinPIC concentration was again determined by CD measurements, and the α CD3 concentration was obtained from a BCA assay. For 0.1, 0.3, 0.5, and 1 equiv of α CD3, an average antibody spacing of approximately 70, 40, 30, and 20 nm was found, respectively. When compared to the average antibody spacing calculated for a coupling efficiency of 100% (50, 17, 10, and 5 nm), it can be concluded that between 25 and 70% of α CD3 antibodies have coupled to the polymer, with a lower coupling efficiency being observed for larger equivalents of

α CD3. This may directly result from the altered DBCO- α CD3-to-azide ratio or originate from steric hindrance, which prohibits access of α CD3 molecules to remaining coupling sites (Figure 4c).

Overall, our results clearly show that the purification of PIC bioconjugates with an affinity tag is a powerful method for obtaining pure bioconjugates in high yield, which can be easily analyzed with standard spectroscopic methods. The affinity-based purification method developed now opens the way toward the synthesis of multifunctional conjugates. The greatly increased yield and purity allow for a step-wise functionalization with different molecules, providing unprecedented control over the number and stoichiometry of functional entities. This method, therefore, represents a highly promising starting point for the further development of PIC bioconjugates for immunotherapeutic applications as well as for designing enzyme cascade reactions, which both require the conjugation of multiple different biomolecules to a polymer scaffold.

CONCLUSIONS

In this study, an affinity-based purification method was developed that increases both the total yield as well as the purity of PIC bioconjugates. PIC polymers were equipped with biotin tags that allow for the reversible binding of the resulting biotinPIC polymers to monoavidin beads. For optimal binding, a minimum statistical spacing between individual biotin moieties of at least 7.5 nm was required. To demonstrate the application potential of this new purification method, two different biotinPIC bioconjugates were successfully synthesized and purified. Although the final yield of the purification was only 10–25%, it was significantly better than the previously used ultrafiltration method, in which the yield was below 1%. The yields of the binding and elution steps may be further optimized when reapplying the supernatant to the monoavidin beads or when using (strept)avidin mutants^{41,42} or biotin derivatives^{43,44} with different affinity. Alternatively, the strong biotin-streptavidin interaction may be utilized when integrating a cleavable linker⁴⁵ between the PIC and the biotin moiety. More importantly, the new method allowed for the removal of nonreacted biomolecules nearly quantitatively (>90%), leading to highly pure biotinPIC bioconjugates. As a consequence of this high purity, the analysis of these constructs was straightforward, and the spacing of the conjugated biomolecules could be calculated from simply dividing the concentration of polymer by the concentration of the respective biomolecule. The densities calculated from bulk concentrations were in good agreement with the results from AFM imaging, in which every individual biomolecule coupled to the polymer was visualized and counted. Furthermore, the developed purification method preserved the activity of the coupled biomolecule as was demonstrated with activity measurements for alkaline phosphatase. Altogether, a new versatile protocol was developed for the synthesis and purification of biotinPIC bioconjugates. This protocol will not only be highly useful for further developing these molecules toward applications but also for the preparation of other complex and multifunctional bioconjugates.

EXPERIMENTAL PROCEDURES

Polymer Synthesis. The PIC polymer used in this study was synthesized according to the procedure described in the literature.^{11,12,14,21,30} In short, a 30:1 ratio of methoxy-

terminated (1.124 g, 3.12 mmol) and azide-terminated (0.0038 g, 0.104 mmol) isocyanopeptide monomers were mixed in toluene (50 mg mL⁻¹) in a round-bottom flask and stirred for 2 days until infrared measurements showed the complete disappearance of the isocyanide peak. The solution was diluted with dichloromethane and precipitated in diisopropyl ether three times, resulting in an off-white solid (0.937 g, 82%). The resulting polymer contains a statistical density of 1 azide per 3 nm. The polymer was analyzed using viscometry as described previously ($M_v = 490$ kg mol⁻¹).¹¹

Biotin Functionalization of PICs. The PIC polymer was dissolved in PBS (10 mM Na₂HPO₄, 2 mM KH₂PO₄, 137 mM NaCl, and 2.7 mM KCl at pH 7.4) in a concentration of 1 mg mL⁻¹. Biotin-EG₄-DBCO (Click Chemistry Tools) dissolved in DMSO or DBCO-PEG₃₀₀₀ Da-biotin (Nanocs) dissolved in DMSO was added to this solution in the required amount (less than 5% of the total volume, see below). The mixture was stirred overnight and subsequently used for testing the monoavidin purification protocol or for the conjugation of biomolecules. A total of four different biotinPIC polymers were prepared with a different density of biotin. To achieve this, the molar ratio of biotin-EG₄-DBCO:monomer was varied from 1:75, 1:100, and 1:400. Assuming a quantitative reaction, this yields an average biotin distance of 7.5, 10, and 40 nm, respectively. During the synthesis of the fourth polymer with a 1:50 molar ratio (5 nm biotin spacing) DIBO-AlexaFluor647 (Thermo Fisher Scientific) was added in a 1:500 ratio of dye to monomer to obtain a fluorescently labeled biotinPIC polymer for testing the migration of biotinPEG in SDS-PAGE (Figure S4). After overnight stirring, the mixture was precipitated in diisopropyl ether and dried in air. The dried material was dissolved in a concentration of 1 mg mL⁻¹ in PBS.

Expression and Purification of PhoA. The *phoA* gene was cloned from the plasmid pET-22b-*phoA*⁴⁶ into a vector of the pAK⁴⁷ and pKB⁴⁸ series, in which the original lac promoter was replaced by the arabinose inducible P_{BAD} promoter. The sequence of the *pelB* signal peptide was replaced with the signal peptide of PhoA. The resulting plasmid pKBS-PhoA-His allows for the periplasmic expression of PhoA with a C-terminal His tag. For protein expression, the plasmid was transformed into the *E. coli* K12 strain TB1 (New England Biolabs). The cultures were grown in SB medium (20 g L⁻¹ tryptone, 10 g L⁻¹ yeast extract, 5 g L⁻¹ NaCl, and 50 mM K₂HPO₄) at 25 °C and induced with 0.02% (w/v) arabinose at an OD₆₀₀ between 0.5 and 1. After 3 h, the cells were harvested by centrifugation at 5000 rpm and 4 °C for 15 min. The cells were resuspended in 50 mM tricine at pH 8.0 and 300 mM NaCl (loading buffer) and lysed using sonication. The lysate was cleared by centrifugation, and the resulting supernatant was incubated at 80 °C for 10 min to denature proteins other than the heat-stable PhoA-His. Denatured proteins were removed by centrifugation (2 × 30 min, 20000g) at 4 °C and filtration through a 0.22 μ m syringe filter. The resulting supernatant was loaded onto a Zn²⁺-NTA column (His Gravi Trap equilibrated with ZnCl₂ instead of NiCl₂; GE Healthcare Life Sciences). Following a washing step with loading buffer (30 column volumes), the column was washed with five column volumes of loading buffer supplemented with 10 mM imidazole. The protein was eluted from the column with 50 mM tricine at pH 8.0, 300 mM NaCl, and 200 mM imidazole. The eluted protein was concentrated using ultrafiltration (10 kDa cutoff; Amicon Ultra-15 centrifugal filter units; Merck Millipore). Lastly, the buffer was exchanged to 50 mM sodium borate pH 8.5 using a

PD-10 desalting column (GE Healthcare Life Sciences). The purity was verified using SDS-PAGE and the correct molecular weight was confirmed with mass spectrometry (ESI-TOF). The protein concentration was determined from its absorbance at 280 nm ($\epsilon = 63260 \text{ M}^{-1} \text{ cm}^{-1}$ for the PhoA dimer) and confirmed using a BCA assay. The purified protein was stored in aliquots at -80°C .

BCA Assay. To determine the protein concentration, a micro-BCA protein assay kit (Thermo Fisher Scientific) was used. The assay was performed using the protocol supplied by the manufacturer. When determining the αCD3 or PhoA–His concentration, non-reacted αCD3 was used as the standard, spanning a concentration range from $7.8 \mu\text{g mL}^{-1}$ to 1 mg mL^{-1} . PIC– αCD3 samples were freeze-dried before the BCA assay and redissolved in PBS to increase the sample concentration by a factor of 5–6.

Synthesis of AlexaFluor647–DBCO–PhoA. PhoA–His ($\sim 15 \mu\text{M}$) was labeled with AlexaFluor647–NHS (Thermo Fisher Scientific) and DBCO– EG_4 –NHS simultaneously (Click Chemistry Tools). Using DMSO stock solutions, 4 equiv of AlexaFluor647–NHS and 4 equiv of DBCO– EG_4 –NHS were added, yielding a final concentration of $60 \mu\text{M}$ for both reagents. The DMSO content was $\sim 10\%$ of the total volume. The reaction was incubated for 3–4 h at 4°C , followed by ultrafiltration with a 10 kDa cutoff. During ultrafiltration, the buffer was exchanged to 50 mM HEPES at pH 8.0. To determine the degree of labeling of the resulting AlexaFluor647–DBCO–PhoA–His, the protein concentration was first determined with a BCA assay. The DBCO and AlexaFluor647 concentrations were determined from UV–vis measurements using an extinction coefficient of $12000 \text{ M}^{-1} \text{ cm}^{-1}$ for DBCO (309 nm) and of $270000 \text{ M}^{-1} \text{ cm}^{-1}$ for AlexaFluor647 (650 nm). This analysis yielded a degree of labeling of 2.5 DBCO and 1.1 AlexaFluor647 molecules per PhoA–His dimer.

Synthesis of αCD3 –DBCO. The αCD3 antibodies (monoclonal mouse antihuman αCD3 clone OKT3; bioXcell) were dissolved in PBS. DBCO– EG_4 –NHS (3.5 equiv in DMSO) was added to the antibody solution. The final concentration of αCD3 in the reaction mixture was 4 mg mL^{-1} . The mixture was stirred for 2 h at 4°C and subsequently purified using ultrafiltration (30 kDa cutoff; Amicon Ultra-15 centrifugal filter units) to remove nonreacted DBCO– EG_4 –NHS. The degree of labeling was determined from absorption measurements at 309 nm (DBCO) and 280 nm (αCD3). The signal at 280 nm was corrected for the absorption of DBCO using the following equation: corrected absorption (280 nm) = absorption at 280 nm – $(1.089 \times \text{absorption at } 309 \text{ nm})$.³⁹ The DBCO concentration was calculated from the absorption at 309 nm ($\epsilon = 12000 \text{ M}^{-1} \text{ cm}^{-1}$). To obtain the αCD3 concentration, the corrected absorption at 280 nm ($\epsilon = 210000 \text{ M}^{-1} \text{ cm}^{-1}$) was used. Typically, this reaction yields a degree of labeling of 2–2.5 DBCO molecules per antibody.

Synthesis of BiotinPIC Bioconjugates. All biotinPIC bioconjugates were prepared using a similar protocol. A solution of biotinPIC (1 mg mL^{-1} stock solution in PBS) was added to the DBCO-functionalized biomolecules to obtain the desired ratios. The reaction mixture was stirred overnight at 4°C and directly used for the purification over monoavidin beads (agarose-based; Thermo Fisher Scientific). PBS was used for the coupling and purification of αCD3 –DBCO. HEPES was used for AlexaFluor647–DBCO–PhoA–His.

Circular Dichroism Measurements. To prepare the CD standard curves, the azide-functionalized PIC was dissolved in a concentration of 1 mg mL^{-1} in PBS (Figure S1). This stock solution was used to prepare the following concentrations of the polymer: 0.025, 0.05, 0.1, 0.2, and 0.3 mg mL^{-1} . The CD spectrum of these samples was measured and corrected using a PBS blank. Standard curves were constructed for the CD signals measured at 272 or 360 nm, yielding calibration factors of $\epsilon_{272 \text{ nm}} = 525.6 \text{ mdeg mL mg}^{-1}$ and $\epsilon_{360 \text{ nm}} = -121.1 \text{ mdeg mL mg}^{-1}$.

Purification Using Monoavidin Agarose. All buffers were freshly prepared and filtered before use. In general, 500–800 μL of a 50% slurry containing regenerated and blocked monoavidin beads was spun down in a Eppendorf tube, and the supernatant was removed. The PIC–biomolecule mixture was added (250–400 μL), and the beads were incubated for 4 h. Following incubation, the beads were spun down, the supernatant was removed, and the remaining beads were washed with PBS containing 0.1% (v/v) Tween 20 (PBS-T, 2 \times) and with PBS (4 \times). The beads were then incubated with PBS containing 2 mM biotin for 1–2 h to release the purified biotinPIC bioconjugate. After affinity purification was completed, the eluted samples were filtered to remove a small portion of remaining beads in the elution fraction. Filtering the samples with standard filters of 0.2–0.45 μm pore size did result in a huge loss of polymer so that a 1 mL column with a frit of 20 μm pore size (Screening Devices) was used instead. Using this larger pore size, the loss of polymer during filtration was reduced to 10%. During all steps of the purification, PBS was used for the PIC– αCD3 bioconjugate, while HEPES was used for the PIC–PhoA samples.

AFM Measurements. The monoavidin purified and filtered PIC–PhoA samples were drop-cast (20 μL) onto freshly cleaved mica. After incubation on the surface for 20 s, the samples were removed, and the surface was dried in a nitrogen stream. The samples were imaged with tapping mode in air using a Nanoscope IV instrument (Bruker) and NSG-10 tapping mode tips (NT-MDT). The images were analyzed with ImageJ software.⁴⁹ The average spacing of PhoA molecules was calculated from the number of enzymes counted on a polymer of given length (Figure S2).

PhoA Activity Measurements. The fluorogenic substrate DDAO–phosphate (9H-(1,3-dichloro-9,9-dimethylacridin-2-one-7-yl) phosphate diammonium salt; Thermo Fisher Scientific) was used for measuring the activity of the biotinPIC–PhoA bioconjugates. The substrate was dissolved in dry DMSO at a concentration of $40 \mu\text{M}$. The biotinPIC–PhoA conjugates were diluted in activity buffer (50 mM HEPES at pH 8.0, 100 mM KCl, 20 mM MgCl_2 , and $100 \mu\text{M}$ ZnCl_2) to obtain a PhoA concentration of 500 pM. DDAO–phosphate was added to a final concentration of $2 \mu\text{M}$ to start the measurement. The release of the fluorophore DDAO was followed in a microplate reader ($\lambda_{\text{ex}} = 620 \text{ nm}$; $\lambda_{\text{em}} = 660 \text{ nm}$; Tecan Infinite M200 PRO). The measurement was performed at 37°C for 40 min (30 s intervals). All measurements were performed in triplicate. The data was corrected for the autohydrolysis of the substrate.

■ ASSOCIATED CONTENT

📄 Supporting Information

The Supporting Information is available free of charge on the ACS Publications website at DOI: 10.1021/acs.bioconjchem.7b00398.

CD calibration curves for the determination of the polymer concentration, SDS-PAGE results of biotinPI-C- α CD3 conjugate, the characterization of the PhoA spacing, and the reaction scheme for the enzymatic conversion of DDAO phosphate. (PDF)

AUTHOR INFORMATION

Corresponding Author

*E-mail: kerstin.blank@mpikg.mpg.de.

ORCID

Kerstin G. Blank: 0000-0001-5410-6984

Present Address

[‡](T.Z.) Department of Pharmacy - Center for Drug Research, Laboratory of Pharmaceutical Biology, University of Munich, Butenandtstr. 5–13, 81377 Munich, Germany.

Author Contributions

[#]R.H. and L.J.E. contributed equally.

Notes

The authors declare no competing financial interest.

ACKNOWLEDGMENTS

The authors thank Florian Hollfelder for providing the plasmid pET-22b-PhoA and Kalyanasundaram Subramanian for cloning the PhoA expression plasmid as well as Reinhild Dünnebacke for PhoA expression and purification. This work was supported by grants from the Dutch Cancer Society (grant nos. KUN2006-3699 and KUN2009-4402), the Dutch government to The Netherlands Institute for Regenerative Medicine (NIRM, grant no. FES0908), The Netherlands Organization for Scientific Research (NWO; Spinoza award 2006, C.G.F.; VICI grant no. 700.56.444, A.E.R.; VIDI grant no. 700.58.430, K.G.B.) as well as NanoNext (grant nos. 7A.06 and 3D.12), the European Research Council (ERC; grant no. ERC-2010-AdG269019, C.G.F.), and the Max Planck Society.

REFERENCES

- (1) Abuchowski, A., van Es, T., Palczuk, N. C., and Davis, F. F. (1977) Alteration of immunological properties of bovine serum albumin by covalent attachment of polyethylene glycol. *J. Biol. Chem.* 252, 3578.
- (2) Harris, J. M., and Chess, R. B. (2003) Effect of pegylation on pharmaceuticals. *Nat. Rev. Drug Discovery* 2, 214.
- (3) Pasut, G., Guiotto, A., and Veronese, F. M. (2004) Protein, peptide and non-peptide drug PEGylation for therapeutic application. *Expert Opin. Ther. Pat.* 14, 859.
- (4) Veronese, F. M., and Pasut, G. (2005) PEGylation, successful approach to drug delivery. *Drug Discovery Today* 10, 1451.
- (5) Boyer, C., Bulmus, V., Liu, J., Davis, T. P., Stenzel, M. H., and Barner-Kowollik, C. (2007) Well-Defined Protein–Polymer Conjugates via in Situ RAFT Polymerization. *J. Am. Chem. Soc.* 129, 7145.
- (6) Gauthier, M. A., and Klok, H.-A. (2008) Peptide/protein-polymer conjugates: synthetic strategies and design concepts. *Chem. Commun.*, 2591.
- (7) Klok, H.-A. (2009) Peptide/Protein–Synthetic Polymer Conjugates: Quo Vadis. *Macromolecules* 42, 7990.
- (8) Cobo, I., Li, M., Sumerlin, B. S., and Perrier, S. (2015) Smart hybrid materials by conjugation of responsive polymers to biomacromolecules. *Nat. Mater.* 14, 143.
- (9) Hoffman, A. S., and Stayton, P. S. (2007) Conjugates of stimuli-responsive polymers and proteins. *Prog. Polym. Sci.* 32, 922.
- (10) Liu, S., Maheshwari, R., and Kiick, K. L. (2009) Polymer-Based Therapeutics. *Macromolecules* 42, 3.
- (11) Mandal, S., Eksteen-Akeroyd, Z. H., Jacobs, M. J., Hammink, R., Koepf, M., Lambeck, A. J. A., van Hest, J. C. M., Wilson, C. J., Blank,

K., Figdor, C. G., et al. (2013) Therapeutic nanoworms: towards novel synthetic dendritic cells for immunotherapy. *Chem. Sci.* 4, 4168.

(12) Mandal, S., Hammink, R., Tel, J., Eksteen-Akeroyd, Z. H., Rowan, A. E., Blank, K., and Figdor, C. G. (2015) Polymer-Based Synthetic Dendritic Cells for Tailoring Robust and Multifunctional T Cell Responses. *ACS Chem. Biol.* 10, 485.

(13) Bennett, N. R., Zwick, D. B., Courtney, A. H., and Kiessling, L. L. (2015) Multivalent Antigens for Promoting B and T Cell Activation. *ACS Chem. Biol.* 10, 1817.

(14) Hammink, R., Mandal, S., Eggermont, L. J., Nooteboom, M., Willems, P. H. G. M., Tel, J., Rowan, A. E., Figdor, C. G., and Blank, K. G. (2017) Controlling T-Cell Activation with Synthetic Dendritic Cells Using the Multivalency Effect. *ACS Omega* 2, 937.

(15) Grotzky, A., Nauser, T., Erdogan, H., Schlüter, A. D., and Walde, P. (2012) A Fluorescently Labeled Dendronized Polymer–Enzyme Conjugate Carrying Multiple Copies of Two Different Types of Active Enzymes. *J. Am. Chem. Soc.* 134, 11392.

(16) Schoffelen, S., and van Hest, J. C. M. (2012) Multi-enzyme systems: bringing enzymes together in vitro. *Soft Matter* 8, 1736.

(17) Wheeldon, I., Minteer, S. D., Banta, S., Barton, S. C., Atanassov, P., and Sigman, M. (2016) Substrate channelling as an approach to cascade reactions. *Nat. Chem.* 8, 299.

(18) Zhu, J. (2010) Bioactive modification of poly(ethylene glycol) hydrogels for tissue engineering. *Biomaterials* 31, 4639.

(19) Zhu, J., and Marchant, R. E. (2011) Design properties of hydrogel tissue-engineering scaffolds. *Expert Rev. Med. Devices* 8, 607.

(20) Kopecek, J., and Yang, J. (2012) Smart Self-Assembled Hybrid Hydrogel Biomaterials. *Angew. Chem., Int. Ed.* 51, 7396.

(21) Das, R. K., Gocheva, V., Hammink, R., Zouani, O. F., and Rowan, A. E. (2016) Stress-stiffening-mediated stem-cell commitment switch in soft responsive hydrogels. *Nat. Mater.* 15, 318.

(22) Velonia, K., Rowan, A. E., and Nolte, R. J. M. (2002) Lipase Polystyrene Giant Amphiphiles. *J. Am. Chem. Soc.* 124, 4224.

(23) Huang, X., Li, M., Green, D. C., Williams, D. S., Patil, A. J., and Mann, S. (2013) Interfacial assembly of protein–polymer nanoconjugates into stimulus-responsive biomimetic protocells. *Nat. Commun.* 4, 2239.

(24) Cornelissen, J. J. L. M., Donners, J. J. J. M., de Gelder, R., Graswinckel, W. S., Metselaar, G. A., Rowan, A. E., Sommedijk, N. A. J. M., and Nolte, R. J. M. (2001) β -Helical Polymers from Isocyanopeptides. *Science* 293, 676.

(25) Schwartz, E., Koepf, M., Kitto, H. J., Nolte, R. J. M., and Rowan, A. E. (2011) Helical poly(isocyanides): past, present and future. *Polym. Chem.* 2, 33.

(26) Koepf, M., Kitto, H. J., Schwartz, E., Kouwer, P. H. J., Nolte, R. J. M., and Rowan, A. E. (2013) Preparation and characterization of non-linear poly(ethylene glycol) analogs from oligo(ethylene glycol) functionalized polyisocyanopeptides. *Eur. Polym. J.* 49, 1510.

(27) Kouwer, P. H. J., Koepf, M., Le Sage, V. A. A., Jaspers, M., van Buul, A. M., Eksteen-Akeroyd, Z. H., Woltinge, T., Schwartz, E., Kitto, H. J., Hoogenboom, R., et al. (2013) Responsive biomimetic networks from polyisocyanopeptide hydrogels. *Nature* 493, 651.

(28) van Buul, A. M., Schwartz, E., Brocorens, P., Koepf, M., Beljonne, D., Maan, J. C., Christianen, P. C. M., Kouwer, P. H. J., Nolte, R. J. M., Engelkamp, H., et al. (2013) Stiffness versus architecture of single helical polyisocyanopeptides. *Chem. Sci.* 4, 2357.

(29) Jaspers, M., Rowan, A. E., and Kouwer, P. H. J. (2015) Tuning Hydrogel Mechanics Using the Hofmeister Effect. *Adv. Funct. Mater.* 25, 6503.

(30) Deshpande, S. R., Hammink, R., Das, R. K., Nelissen, F. H. T., Blank, K. G., Rowan, A. E., and Heus, H. A. (2016) DNA-Responsive Polyisocyanopeptide Hydrogels with Stress-Stiffening Capacity. *Adv. Funct. Mater.* 26, 9075.

(31) Hochuli, E., Bannwarth, W., Dobeli, H., Gentz, R., and Stuber, D. (1988) Genetic Approach to Facilitate Purification of Recombinant Proteins with a Novel Metal Chelate Adsorbent. *Nat. Biotechnol.* 6, 1321.

(32) Schmidt, T. G. M., and Skerra, A. (2007) The Strep-tag system for one-step purification and high-affinity detection or capturing of proteins. *Nat. Protoc.* 2, 1528.

(33) Wu, S.-C., and Wong, S.-L. (2006) Intracellular production of a soluble and functional monomeric streptavidin in *Escherichia coli* and its application for affinity purification of biotinylated proteins. *Protein Expression Purif.* 46, 268.

(34) Green, N. M., and Toms, E. J. (1973) The properties of subunits of avidin coupled to Sepharose. *Biochem. J.* 133, 687.

(35) Henrikson, K. P., Allen, S. H. G., and Maloy, W. L. (1979) An avidin monomer affinity column for the purification of biotin-containing enzymes. *Anal. Biochem.* 94, 366.

(36) Debets, M. F., van Berkel, S. S., Schoffelen, S., Rutjes, F. P. J. T., van Hest, J. C. M., and van Delft, F. L. (2010) Azadibenzocyclooctynes for fast and efficient enzyme PEGylation via copper-free (3 + 2) cycloaddition. *Chem. Commun.* 46, 97.

(37) Kitto, H. J., Schwartz, E., Nijemeisland, M., Koepf, M., Cornelissen, J. J. L. M., Rowan, A. E., and Nolte, R. J. M. (2008) Post-modification of helical dipeptido polyisocyanides using the 'click' reaction. *J. Mater. Chem.* 18, 5615.

(38) Leira, F., Vieites, J. M., Vieytes, M. R., and Botana, L. M. (2000) Characterization of 9H-(1,3-dichloro-9,9-dimethylacridin-2-ona-7-yl)-phosphate (DDAO) as substrate of PP-2A in a fluorimetric microplate assay for diarrhetic shellfish toxins (DSP). *Toxicon* 38, 1833.

(39) Kotagiri, N., Li, Z., Xu, X., Mondal, S., Nehorai, A., and Achilefu, S. (2014) Antibody Quantum Dot Conjugates Developed via Copper-Free Click Chemistry for Rapid Analysis of Biological Samples Using a Microfluidic Microsphere Array System. *Bioconjugate Chem.* 25, 1272.

(40) Hvasanov, D., Nam, E. V., Peterson, J. R., Pornsaksit, D., Wiedenmann, J., Marquis, C. P., and Thordarson, P. (2014) One-Pot Synthesis of High Molecular Weight Synthetic Heteroprotein Dimers Driven by Charge Complementarity Electrostatic Interactions. *J. Org. Chem.* 79, 9594.

(41) Malmstadt, N., Hyre, D. E., Ding, Z., Hoffman, A. S., and Stayton, P. S. (2003) Affinity Thermoprecipitation and Recovery of Biotinylated Biomolecules via a Mutant Streptavidin-Smart Polymer Conjugate. *Bioconjugate Chem.* 14, 575.

(42) Laitinen, O. H., Hytönen, V. P., Nordlund, H. R., and Kulomaa, M. S. (2006) Genetically engineered avidins and streptavidins. *Cell. Mol. Life Sci.* 63, 2992.

(43) Hofmann, K., Wood, S. W., Brinton, C. C., Montibeller, J. A., and Finn, F. M. (1980) Iminobiotin affinity columns and their application to retrieval of streptavidin. *Proc. Natl. Acad. Sci. U. S. A.* 77, 4666.

(44) Hirsch, J. D., Eslamizar, L., Filanoski, B. J., Malekzadeh, N., Haugland, R. P., Beechem, J. M., and Haugland, R. P. (2002) Easily reversible desthiobiotin binding to streptavidin, avidin, and other biotin-binding proteins: uses for protein labeling, detection, and isolation. *Anal. Biochem.* 308, 343.

(45) Leriche, G., Chisholm, L., and Wagner, A. (2012) Cleavable linkers in chemical biology. *Bioorg. Med. Chem.* 20, 571.

(46) Huebner, A., Olguin, L. F., Bratton, D., Whyte, G., Huck, W. T. S., de Mello, A. J., Edel, J. B., Abell, C., and Hollfelder, F. (2008) Development of Quantitative Cell-Based Enzyme Assays in Microdroplets. *Anal. Chem.* 80, 3890.

(47) Krebber, A., Bornhauser, S., Burmester, J., Honegger, A., Willuda, J., Bosshard, H. R., and Plückthun, A. (1997) Reliable cloning of functional antibody variable domains from hybridomas and spleen cell repertoires employing a reengineered phage display system. *J. Immunol. Methods* 201, 35.

(48) Blank, K., Morfill, J., Gump, H., and Gaub, H. E. (2006) Functional expression of *Candida antarctica* lipase B in *Escherichia coli*. *J. Biotechnol.* 125, 474.

(49) Schneider, C. A., Rasband, W. S., and Eliceiri, K. W. (2012) NIH Image to ImageJ: 25 years of image analysis. *Nat. Methods* 9, 671.